The Measurement of Very Low Conductivity and Dielectric Loss in XLPE Cables:
A Possible Method to Detect Degradation due to Thermal Aging

J.C. Fothergill[1], T. Liu[2], S.J. Dodd[1], L.A. Dissado[1], U.H. Nilsson[3]
1: Dept. of Engineering, University of Leicester, Leicester, LE1 7RH, UK
2: Electric Power Research Institute of China Southern Power Grid, Guangzhou, P.R.China, 510080
3: Borealis AB, Innovation Centre, 44 486 Stenungsund, Sweden

The dielectric response of crosslinked polyethylene (XLPE) insulated, miniature power cables, extruded with inner and outer semicons, was measured over the frequency range 10^{-4} to 10^{4} Hz at temperatures from 20 to 100°C. A dielectric spectrometer was used for the frequency range 10^{-4} to 10^{-2} Hz. A bespoke noise-free power supply was constructed and used to measure the DC conductivity and, using a Fourier transform technique, it was also used to measure the very low dielectric tanδ losses encountered at frequencies of 1 to 100 Hz. Tanδ measurements of $<10^{-5}$ were found in this frequency range and attributed to a β-mode dielectric relaxation lying above 100 Hz due to motion of chain segments in the amorphous region and an α-mode relaxation lying below 1 Hz window due to twists of chains in the crystal lamellae. The DC conductivity measurements were consistent with those of the dielectric spectrometer and indicate lower DC conductivities in vacuum degassed cables than have been previously reported for XLPE (less that 10^{-17} S.m^{-1}). The conduction process is thermally activated with an activation energy of approximately 1.1 eV. Higher conductivities were found for non-degassed cables. A transformer ratio bridge was used for measurements in the range 1 to 10 kHz; loss in this region was shown to be due to the series resistance of the semicon layers. Thermal ageing of the cables at 135°C for 60 days caused significant increases in the conductivity and tanδ and it is considered that such measurements may be a sensitive way of measuring electrical degradation due to thermal aging.

***Index Terms*— Crosslinked polyethylene, power cables, conductivity, dielectric loss, thermal aging**

I. Introduction

Polyethylene in its crosslinked form (XLPE) is widely used as an electrical insulator in extruded power cables. Since such cables may be required to conduct currents of several kA and support hundreds of kV, they form critical parts of the transmission infrastructure (e.g. [1]) and are expected to be highly resilient to failure (e.g. the National Grid Company requires high voltage power cable systems to have an operating life of at least 40 years [2].) It is therefore crucial to be able to assess whether such cables have been electrically degraded due to thermal ageing, and yet no such assessment technique is widely accepted. This paper shows that the measurement of the DC conductivity, and possibly tanδ, difficult though such measurements may be, could be used for the assessment of such ageing.

Furthermore, the characterization of the DC conductivity and the low frequency dielectric characteristics of XLPE cables as functions of temperature and field are becoming increasingly important as such cables find a greater prevalence in high-voltage DC transmission. Such systems are being installed, *inter-alia*, for long-distance transmission for pan-continental power lopping and for connecting often remote sustainable power sources to centers of population (e.g. [3]).

Whilst measurements of the conductivity and low-frequency dielectric response of polyethylene have been widely reported (e.g. [4,5]), there have been considerable variations: for example, the UK National Physical Laboratory gives a wide range of conductivities for polyethylene [6] from 10^{-13} to 10^{-16} S.m^{-1}. In this paper we confirm measurements of the very low frequency dielectric characteristics by using two different techniques, which give results that are in agreement. One of these, the measurement of DC conductivity, uses a bespoke, virtually noise-free, highly stable DC supply. Samples in the form of long miniature model power cables, which have a high ratio of area to thickness, have been used to make it possible to measure conductivities and dielectric losses with lower noise levels than previously reported for XLPE cables.

Using such samples we have also been able to probe the very low loss dielectric polarization mechanisms occurring close to the power frequencies and have found values of tanδ lower than 10^{-5}. Conductivities as low as 10^{-17} S.m^{-1} have been measured.

II. Dielectric Theory

We would expect the real part of the permittivity (ε') of XLPE to remain reasonably constant over the frequency range studied (10^{-4} to 10^{4} Hz) and not to be particularly influenced by electric field strength in the range up to ~1 kV.mm^{-1} that was used. The dielectric loss (tan δ) would therefore tend to have the same trends with frequency as the imaginary component of the permittivity (ε'') since $\tan\delta = \varepsilon''/\varepsilon'$.

A. Low Frequency Behavior

At very low frequencies, perhaps less than 1 Hz, DC conduction may dominate the dielectric loss. If the polarization mechanisms are independent of frequency in this frequency range, then the cable insulation may be represented by a parallel conductance, *G,* and capacitance, *C*, Figure 1.

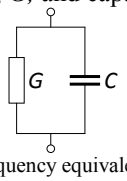

Figure 1: Possible low-frequency equivalent circuit of cable insulation

The impedance, **Z**, of this circuit may be found using equation (1)

$$\frac{1}{\mathbf{Z}} = G + \mathbf{j}\omega C \tag{1}$$

Rather than considering such a complex impedance, it is conventional in dielectric spectroscopy to consider a complex capacitance; this is given the symbol **C*** to distinguish it from the (scalar) capacitance *C* of the cable that is due to the polarization of the dielectric. Since in general the impedance of a capacitor is $1/\mathbf{j}\omega C$, the complex capacitance of Figure 1 can be written as:

$$\mathbf{j}\omega\mathbf{C}^* = \frac{1}{\mathbf{Z}} = G + \mathbf{j}\omega C \text{ or}$$

$$\mathbf{C}^* = C - \mathbf{j}\frac{G}{\omega} \tag{2}$$

The loss tangent at very low frequencies is therefore:

$$\tan\delta = \frac{C''}{C'} = \frac{G}{\omega C} = \frac{1}{\omega R_P C} \tag{3}$$

where R_P is the parallel resistance equivalent to $1/G$.

At low frequencies, the imaginary term, G/ω, will dominate and so, if Figure 1 is a reasonable low-frequency equivalent circuit of the cable, the measured imaginary capacitance, and hence the imaginary permittivity, and hence the tan δ, will be inversely proportional to frequency. The real part of the permittivity will be constant.

B. Behavior at High and Low Frequencies

At higher frequencies, the capacitance of the cable will cause a significant current to be drawn. In extruded power cables it is necessary to have a very smooth interface between the insulation and the conductor since conductor asperities protruding into the insulation would cause high field regions that may lead to premature breakdown (e.g. [7]). A (semi-) conducting polymer is therefore extruded over the inner conductor, known as the inner semicon. Similarly an outer semicon is extruded over the polymer insulation and is in contact with the outer conductor, which is normally at earth potential. At high frequencies, the displacement current drawn by the capacitive cable, may cause a potential to be dropped across these semicons, which form a series resistance, R_S, with the capacitance of the cable, Figure 2 [8]. (In this figure, R_P is the reciprocal of the conductance of the cable insulation, i.e. *G* in Figure 1)

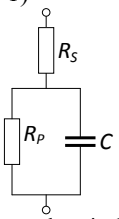

Figure 2: More general equivalent circuit of cable

The impedance, **Z**, of this circuit shown in Figure 2 is

$$\mathbf{Z} = Z' + \mathbf{j}Z''$$
$$= \frac{R_P + R_S\left(1+\omega^2 R_P^2 C^2\right)}{(1+\omega^2 R_P^2 C^2)} - \mathbf{j}\frac{\omega R_P^2 C}{(1+\omega^2 R_P^2 C^2)} \tag{4}$$

The full expression for the loss tangent is therefore:

$$\tan\delta = \frac{Z'}{Z''} = \frac{R_P + R_S\left(1+\omega^2 R_P^2 C^2\right)}{\omega R_P^2 C}$$
$$= \omega R_S C + \frac{R_P + R_S}{\omega R_P^2 C}$$
$$\cong \omega R_S C + \frac{1}{\omega R_P C} \text{ (since } R_P >> R_S\text{)}$$
$$= \frac{\omega}{\omega_S} + \frac{\omega_P}{\omega}$$
$$\text{where } \omega_S = \frac{1}{R_S C} \text{ and } \omega_P = \frac{1}{R_P C} \tag{5}$$

Since $R_S << R_P$, $\omega_S >> \omega_P$ and therefore $\tan\delta \propto \omega^{-1}$ at lower frequencies (< ~1 Hz) and $\tan\delta \propto \omega^{+1}$ at higher frequencies. This is shown schematically in Figure 3.

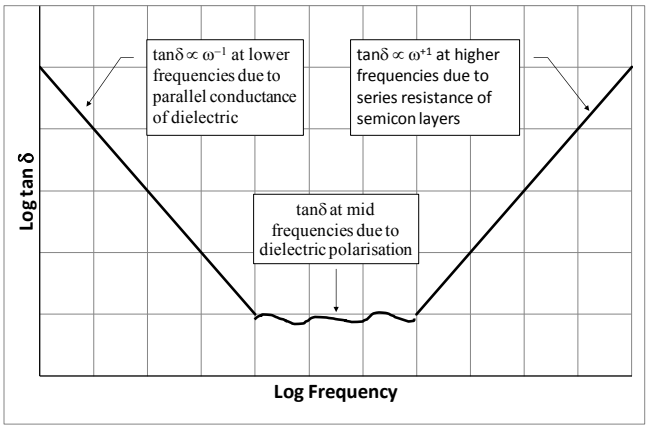

Figure 3: Schematic of expected tan δ response of cable

III. SAMPLES

Samples were manufactured by the Borealis Innovation Centre (Stenungsund, Sweden) in the form of miniature "model" power cables. These three-layer coaxial cables were extruded on a 1+2 pilot cable line. In this line, the conductor is first drawn through a single extruder head, which forms the inner semicon layer. This is immediately followed by double

extrusion head in which the insulation and outer semicon layers are formed. The polyethylene insulation and semicon layers are dry cured (crosslinked) in a vulcanization tube of a conventional catenary continuous vulcanization (CCV) cable line. A photograph of the end of such a cable is shown in Figure 4.

The cables were tested either:

- *as received*, or
- *air degassed* by keeping them in a normal oven at 80°C for 5 days, or
- *vacuum degassed* by further degassing them in a vacuum oven (<10^2 Pa) at 80°C for another 5 days.

The degassing was intended to remove the crosslinking byproducts. In a normal power cable, these byproducts may diffuse out of the system naturally, typically over the first few months of operation. The peroxide byproduct levels, measured by Borealis using high-performance liquid chromatography (HPLC), before and after these degassing processes are shown in Table 1.

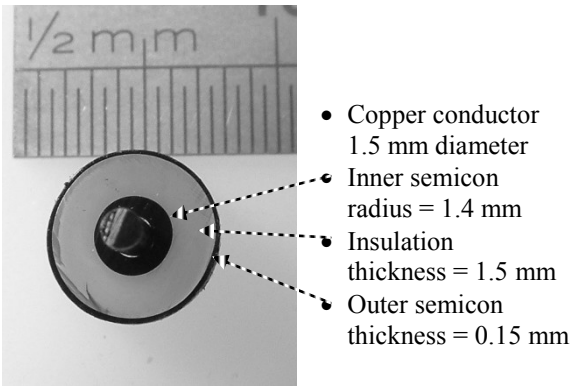

Figure 4: Miniature Power Cables used as samples

TABLE 1: PEROXIDE BY-PRODUCTS IN PPM (MASS) AFTER DEGASSING REGIMES

	As received	*Air degassed*	*Vacuum degassed*
Dicumyl peroxide	<100	< 100	< 100
Acetophenone	2927	< 100	< 100
Alpha methyl styrene	<100	< 100	< 100
Cumyl alcohol	4923	125	< 100

In order to study the ageing effects, some of the degassed cable samples underwent an accelerated thermal ageing regime of 135°C for 60 days (1440 hours) [9]. In Figure 5, the effect of ageing on cables without an outer semicon layer can be observed. The color of the XLPE insulation layer changed from translucent grey to a rich, less transparent, brown, which is presumably indicative of thermo-oxidative degradation likely to occur under these circumstances [10]. It has been reported that, as well as an expected change in coloration, this ageing may lead to an increase in free volume and the mobility of charge carriers [10].

Figure 5: Comparison of aged (top) and un-aged model power cables.

In order to reduce leakage currents across the surface of the ends of the cable, guard rings were cut in the outer electrodes close to the ends. The active length of the cable, i.e. between the guard rings, was 5±0.01 m. In order to reduce the resistance of the connection to the outer semicon, the semicon was covered with a copper tape that had a conductive adhesive. Other techniques that were tried included lapping the outer semicon with copper tape without an adhesive, and winding copper wire tightly around the outer semicon. However, these were unsuccessful as the resistance of the connection to the outer semicon was greater than that of the semicon itself. (For the samples used here, the outer semicon resistance could have been as low as 0.02 Ω at low temperatures.) The cable, prepared in this way, is shown in Figure 6.

Figure 6: Miniature cable prepared for testing.

The conductance and capacitance of a cable are proportional to $L/\ln(r_o/r_i)$, where L is the cable length and r_o and r_i are outer and inner radii of the insulation. For these

cable samples, $L/\ln(r_o/r_i) = 6.87$ m. For comparison, a plaque of the same thickness (1.5 mm) and conductance or capacitance would have an area of 0.0647 m^2, e.g. a square of side approximately 254 mm. This would normally be considered a large area to thickness ratio.

IV. Experimental

Three sets of equipment were used for characterization of the samples.

A. Dielectric Spectrometer

A Solartron 1255 Frequency Response Analyzer (FRA) with CDI interface was used to measure real and complex capacitance under computer control. The sample was maintained at a constant temperature (±0.1 C) in a fan oven during the measurements. The excitation voltage was 1.00 V RMS. An air capacitor, of similar capacitance to the cable, was used to establish the noise floor for these measurements. This is shown as a tanδ spectrum in Figure 7; the instrument was not reliable in the filled area. This was found to restrict the use of the instrument to low frequencies (<<1 Hz), and often then only at elevated temperatures.

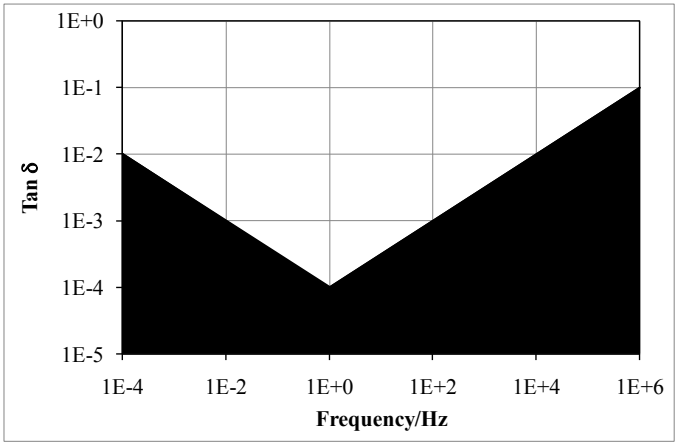

Figure 7: Noise floor for Dielectric Spectrometer; the instrument was not reliable in the grayed area

B. Charging – Discharge Current Measurements

A bespoke power supply was also developed. This was originally used with a model 6485 Keithley picoammeter for measuring the conduction current. However, given the limitation of the dielectric spectrometer, it was also necessary to measure charging and discharging currents to implement time domain dielectric spectroscopy at frequencies corresponding to the lowest dielectric losses. After transformation into the frequency domain these measurements resulted in calculations of the real and imaginary capacitance up to frequencies of 100 Hz. The response of the picoammeter was insufficiently rapid for these measurements, and so a current-to voltage converter was constructed using an electrometer-grade operational amplifier, and the output of this was fed to a digitizing oscilloscope.

The output of commercial high-voltage DC power supplies may drift with time and may also contain high-frequency ripple. Such ripple, especially in older (analogue) supplies may be predominantly at the mains power frequency; in more modern switch-mode supplies, this may occur at higher frequencies, typically around 20 kHz. If the sample is considered to be equivalent to a resistor, R, in parallel with a capacitor, C, then the current flowing through the sample can be usefully calculated as the sum of the components due to the steady-state applied voltage, V, the voltage drift, dV/dt, and the RMS ripple voltage, V_r. The components of current, after switching transients have died away, are:

$$\text{Conduction current:} \quad I_c = \frac{V}{R} \tag{6}$$

$$\text{Current due to voltage drift:} \quad I_d = C\frac{dV}{dt} \tag{7}$$

$$\text{RMS current due to ripple voltage:} \quad I_r = 2\pi f C V_r \tag{8}$$

Even with the relatively high value of $L/\ln(r_o/r_i)$ calculated above, the resistance of the cable samples sometimes exceeded $10^{15}\,\Omega$. For a 1 kV DC supply voltage, this resulted in conduction currents to be measured of less than 10^{-12} A. The capacitance of the cable sample was approximately 850 pF. For the current due to the voltage drift to be less than the conduction current that was required to be measured, $C.dV/dt$ had to be less than 10^{-12} A. The voltage drift therefore had to be less than 1 V in 850 s (i.e. about quarter of an hour.) This may be quite difficult for a supply that is heating up or in a laboratory in which the temperature changes during the day and night.

Whilst the current due to voltage ripple may be, to some extent, filtered out, it is still desirable for this to be not significantly greater than the conduction current to be measured. For 50 Hz ripple, this implies a ripple voltage less than a few μV; for 20 kHz ripple, a ripple voltage of less than 10 nV would be required. Figure 8 shows a typical charging current measured using a conventional HV supply.

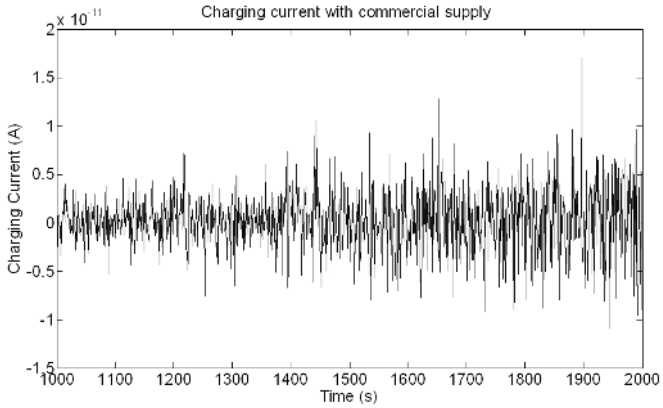

Figure 8: Current measured using a conventional HV supply

For time domain dielectric spectroscopy, it was necessary to switch the voltage source output to a short circuit rapidly; for frequencies of 100 Hz this must occur in less than 10 ms. This is not usually possible with commercially available high-voltage supplies.

A simple high-voltage supply was therefore designed using 120 series-connected batteries, each nominally 9 V, to give an approximate output voltage of 1 kV. A potential divider was used to monitor the voltage. A toggle switch connected the output to either the battery supply or earth; it was found that this switched the output voltage in less than 200 μs. Since very little load is drawn from the batteries, they last a very long time and their output voltage is reasonably constant. With this supply, there are no high frequency harmonics in the output voltage. The only source of voltage fluctuation is from changes in ambient temperature. The temperature dependence of the 1kV supply is estimated from Figure 9 to be 3.2 V/°C. The temperature of the supply therefore had to be maintained to within 0.3 °C over a 15 minute period. Since the batteries had a large thermal mass and were well thermally insulated, this was not problematic.

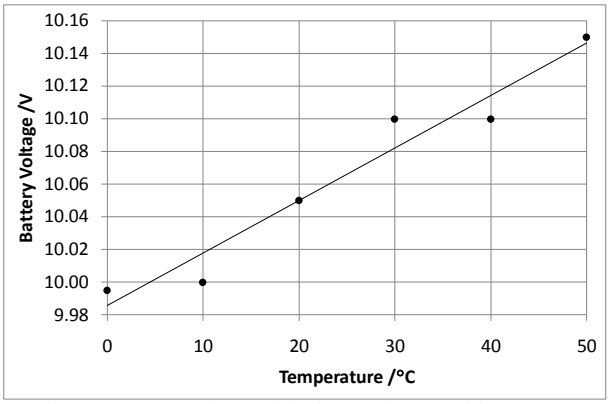

Figure 9: Output voltage of single "9V" battery with temperature

The basic circuit used for charging – discharging current measurements is shown in Figure 10. For time-domain dielectric spectroscopy, the current from the cable, rather than being fed into a picoammeter, was fed into two current-to-voltage converters. One of these was set to a high gain but had a lower bandwidth, the other had a lower gain but a higher bandwidth. The voltage outputs from these were measured by a digital oscilloscope connected to a PC. The lower-gain higher-bandwidth converter measurements were used for the initial discharge measurements in which the current is dropping rapidly from a higher value typically in the first few tens of milliseconds. The other converter was used to capture the lower current measurements for the following second or so of time. These time-domain measurements were transformed to the frequency domain using a Fast Fourier Transform (FFT) technique [11]. For lower frequency measurements the dielectric spectrometer was used for the dielectric response and the picoammeter was used for conduction current measurements.

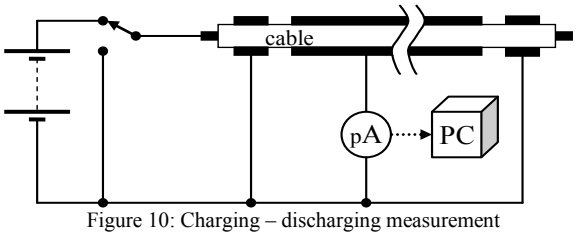

Figure 10: Charging – discharging measurement

C. *Transformer Ratio Bridge*

A transformer ratio bridge was constructed by adapting a Wayne Kerr universal bridge B221, normally used for a frequency of 10^4 rad/s (1592 Hz). A variable frequency sinusoidal signal generator was used to supply the voltage transformer and a tuned amplifier coupled to an oscilloscope was used as a detector. This is shown in Figure 11. If the symmetrical tappings are chosen on the voltage transformer, then the standard impedance is adjusted until a null is detected at which point the two impedances are identical. Different tappings can extend the range of the instrument. In practice the transformer core magnetically saturated below the frequency for which it was designed so, only the results at or above this frequency were used.

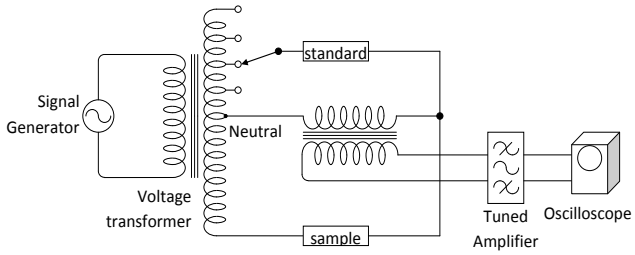

Figure 11: Transformer Ratio Bridge

V. Results and Discussion

A. *Overall Dielectric Response*

Figure 12 attempts to present the overall cable response at 80°C. The measured points using the Frequency Response Analyser (FRA) are shown as circles at the lower frequencies. The unfilled circles were shown, using the air capacitor, to be dominated by noise, whereas the filled circles are considered to be true measurements. The dashed line apparently connecting these points is, in fact, the line corresponding to the estimate of tanδ due to the measured conduction current using the low-noise supply and picoammeter. There is therefore excellent agreement between these two independent methods of measuring conductance despite the difference in electric fields (3 V rms for the dielectric spectrometer, 1000 V for the power supply, over a thickness of 1.5 mm.)

The gray dots are calculated values of tanδ using the fast Fourier transform of the discharge current – i.e. the time domain dielectric spectroscopy described at the end of section IV.B. It is important to note that these points do not include the dielectric loss due to the conduction current (since they are based on measurements of the discharge current.) These represent very low values of tanδ, which would be very difficult to measure using any other technique.

The triangles show measurements using the modified transformer ratio bridge. The bridge appears to give reasonable results down to around 2 kHz, below which magnetic saturation of the transformer core means that the measurements are essentially noise. Again these are distinguished by filled and unfilled symbols. The dot-dash line through the solid triangles has a slope of +1, indicating the expected relationship between tanδ and frequency if this is dominated by the series resistance of the semicon layers.

There appears to be a reasonable agreement between the slope of this estimate and the results of the transformer bridge.

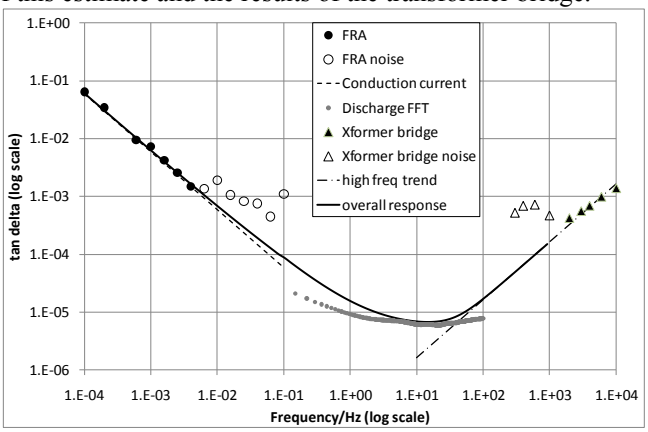

Figure 12: Overall dielectric response at 80°C

The solid line shows an estimated overall response. In order to construct this line the individual responses due to conduction current, polarization loss, and high frequency loss due to the semicons have been considered. The conduction loss used was the $G/\omega\varepsilon'$ line since this agreed so well with the FRA data. For the polarization loss (i.e. that calculated from the FFT of the discharge current) a polynomial fit was used to characterize the data. Since this FFT data did not include the conduction losses, these two losses were added. The loss associated with the semicons was fitted using the best fit to the reliable transformer bridge measurements with a slope of +1 (corresponding to $\tan\delta \propto \omega^{+1}$, equation (5)). The estimated overall response follows this asymptote at higher frequencies. There is clearly some inaccuracy here which may be caused by the FFT being less accurate at higher frequencies or inaccuracies in the transformer ratio bridge. The tan delta may therefore be somewhat lower around 30 to 100 Hz; there is some uncertainty in this region. The minimum loss of $\tan\delta \approx 6\times10^{-6}$ occurs in this region, i.e. close to the common power frequencies of 50 or 60 Hz.

At lower temperatures it is no longer possible to measure the low-frequency conductivity using the FRA, but more of the polarization loss is revealed Results for 60°C, as well as 80°C, are shown in Figure 13.

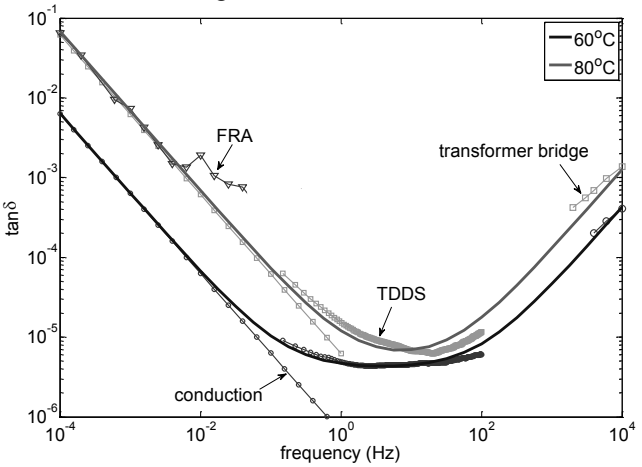

Figure 13: Dielectric response at 60°C and 80°C

B. Conduction and Low Frequency Characteristics

Using the noise-free supply and picoammeter to measure conduction current and verifying the measurements using low-frequency dielectric spectroscopy where possible, measurements were made of conductivity under a range of conditions. Two XLPE insulated cables ("A" and "B") were measured, which had different LDPE base resins. Measurements were made at 20, 40, 60 and 80°C. Conductivities were measured both before and after aging. In all cases the cables were vacuum degassed. The results are presented as Arrhenius plots in Figure 14. The conductivities measured, especially at low temperatures, are extremely small ($\sim 10^{-17}\ \Omega^{-1}\text{m}^{-1}$) and follow good straight lines on this plot, indicating that the measurement techniques were accurate and with low noise.

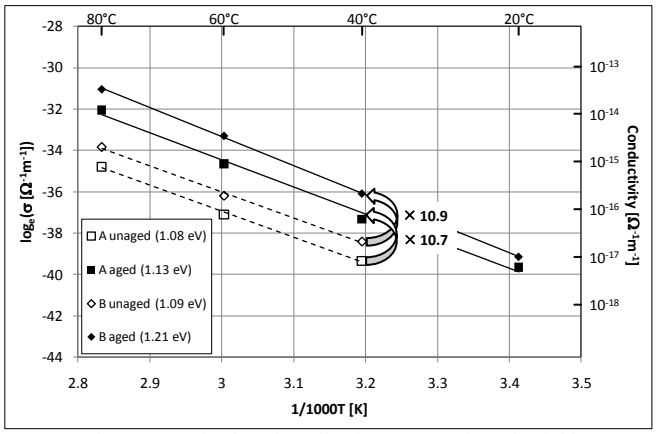

Figure 14 Arrhenius Plots showing measured conductivities. Two types of XLPE cables were used ("A" = squares, "B" = diamonds). Cables were unaged (unfilled symbols) and aged (filled)

Cable B had higher conductivity values than cable A by about 40%, so it is clear that the type of base resin is critical in controlling the conductivity. The activation energies for four cases (two cables, aged and unaged) were close to 1.1 eV; it is possible that the aging slightly increased the activation energy although this cannot be stated with any statistical confidence.

Degassing reduced the conductivity significantly. This is shown in Figure 15 for the case of Cable A. For the sake of clarity, cable B is not shown in this figure, however, the effect of degassing was even more significant in that case. The vacuum degassed and air degassed values are virtually identical thereby demonstrating: (i) the vacuum degassing was no more effective in removing conducting species than the air degassing, (ii) the excellent repeatability of the conductivity measurements.

It is interesting to speculate whether the charge carriers are the same in the fresh and degassed cables. Whilst we would expect the mobility of the carriers to be temperature dependent, we would not expect this to be changed because of the degassing procedure – the material is not itself significantly changed. There are two possible scenarios:

Scenario 1: The charge carriers in the degassed material are the same as in the fresh material – their concentration has just been reduced. In this case we have:

$$\sigma = n.e.\mu(T)$$
$$\text{and } \sigma_{fresh} > \sigma_{degassed} \text{ because } n_{fresh} > n_{degassed} \quad (9)$$

We would expect the relationship of conductivity with temperature to remain unchanged.

Scenario 2: In the fresh material there are volatile additives which are removed by the degassing. These volatiles act as extra charge carriers. In this case we have:

$$\begin{aligned}\sigma_{fresh} &= \sigma_1 \text{ (due to carriers that remain after degassing)} \\ &\quad + \sigma_2 \text{ (due to carriers removed by degassing)} \\ &= n_1.e.\mu_1(T) + n_2.e.\mu_2(T)\end{aligned} \quad (10)$$

In this case, n_1, the concentration of the "indigenous" charge carriers, is the same in both the fresh and degassed materials. The extra carriers, which are removed by the degassing, have concentration n_2 and mobility μ_2. The temperature dependencies of the mobilities of these two species of carriers, i.e. their activation energies, are likely to be different.

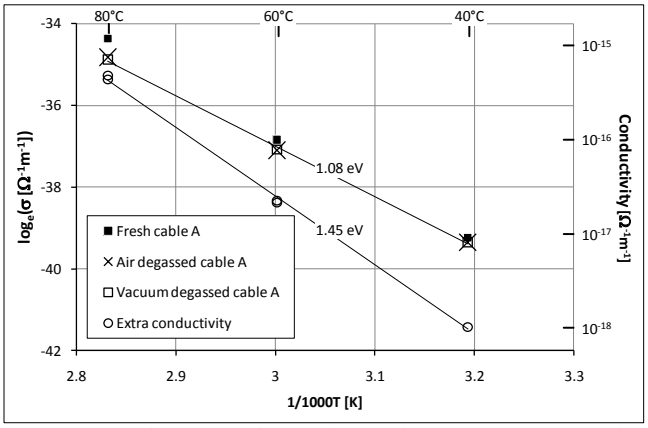

Figure 15: Arrhenius plot showing $\log_e$ conductivity versus reciprocal temperature (1000/T) for fresh and degassed cables. The "reduced conductivity" data presented is both that for air and vacuum degassing.

In Figure 15, the reduction in conductivity, caused by degassing the cables is also shown (denoted as 'extra conductivity'). This conductivity is plotted for cable A together with the conductivity for the fresh cable (solid squares), the vacuum degassed cable (open squares) and air degassed values (crosses). (There is remarkably good agreement between the two degassed samples.) Also shown is the extra conductivity found in fresh cables compared to the degassed values. It can be seen that this extra conductivity has a much higher activation energy than that of the vacuum degassed samples. This therefore corresponds to σ_2 in scenario (2), in which there is an extra species of carriers in the fresh cable that are removed during degassing, and which have a different temperature-dependent mobility than that of the carriers indigenous to the XLPE. The higher activation energy would tend to support the carriers being physically bigger and more difficult to move through the material. It may be possible that the volatile species are ionized, and move through the material. This is consistent with space charge measurements on XLPE cables in which the effect of the concentration of antioxidant and acetophenone has been studied (e.g. [12]).

Aging caused the conductivity to increase by just over an order of magnitude (at 40°C). Nedjar [10] reported on conductivity changes upon aging 2mm thick plaques of XLPE (Union Carbide 4201 with Santonox anti-oxidant) at several temperatures in ventilated ovens. Measurements of conductivity were not made in the steady state but after 2 minutes of the application of 500 V, and so were higher than those measured here. Before ageing it was found that this technique yielded a conductivity of between 3×10^{-12} and $5.5\times10^{-12}\,\Omega^{-1}\text{m}^{-1}$. After ageing at 120°C and 140°C, this value increased to 67×10^{-12} and $142\times10^{-12}\,\Omega^{-1}\text{m}^{-1}$ respectively, an increase of a factor of 20 to 25. This was attributed to a weakening of molecular bonds and in an increase in free volume. It was stated that "This phenomenon leads to an increase in the mobility of the charge carriers along with a reduction in the volume resistivity."

Fothergill *et al* [13] published work on the change of conductivity of full-sized cables electro-thermally aged as part of the EU ARTEMIS project [14]. These cables had an insulation thickness of 18 mm and were aged at 90 kV rms for 6 months (4380 h) at a temperature of 80°C. The results of this work are shown in Figure 16 alongside the results from the current work. It is clear that there is good correspondence in conductivity for the unaged cables, although the current improvements in experimental techniques have allowed measurements at lower conductivities and hence lower temperatures. The ageing in the ARTEMIS project was considerably less harsh than in the current work, indeed the conditions used would probably not have used up all the antioxidant. It is therefore unsurprising that the effect of the ARTEMIS ageing on the conductivity, as seen in Figure 16, was considerably less than that of the ageing in the current work.

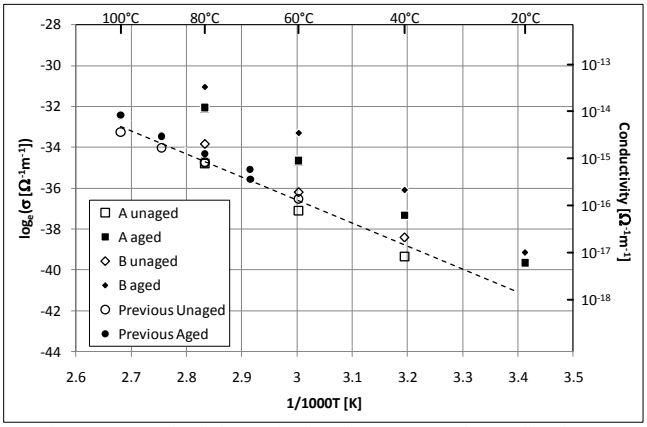

Figure 16: Conductivity Arrhenius plots compared to earlier data [13]. The symbols are as Figure 14 with circles for the earlier data The dashed line is the best fit for all unaged data.

C. Dielectric Loss at Mid-Range (Power) Frequencies

The FFT (time-domain) technique allowed measurements of very low dielectric losses in the frequency range 0.1 to 100 Hz which did not include the loss due to DC conduction. This showed very broad dielectric losses, shown as a function of temperature in Figure 17.

Scarpa *et al* [5] studied the dielectric response of XLPE cable submerged in water, over the frequency range 10^{-5} to 10^{6} Hz. Whilst they did not make measurements in the range 0.1 to 10 Hz, they fitted a broad peak to the imaginary susceptibility in this region using Jonscher's "universal" relaxation law (e.g. [15]) of the form:

$$\chi''(\omega) = \frac{2\chi''_{\max}}{(\omega/\omega_p)^{-m} + (\omega/\omega_p)^{1-n}} \quad (11)$$

For unaged cable, Scarpa *et al* appear to have found values corresponding to:

$$\chi''_{\max} = 8\times10^{-4}, \quad \omega_p/2\pi = 2\,\text{Hz}, \quad m = 0.32, \quad 1-n = 0.2$$

The values of m and $1-n$ indicate the slopes of the peak at frequencies respectively lower and higher than the peak frequency, $\omega_p/2\pi$; their low values indicate that the peak is very broad. This peak (shown as tanδ rather than χ'') is also shown in Figure 17. Although their results, which were at "room temperature", are an order of magnitude bigger than those presented here, the breadth of the peak is in agreement with our data. In contrast our results are over an order of magnitude smaller and show the overlap between a high and low frequency loss response (with peaks that lie outside of the frequency window of 0.1 – 100 Hz) rather than the loss peak obtained at 'room temperature' in [5]. The value of tanδ in our measurements is low enough to correspond to the intrinsic loss processes of the XLPE, in which case [16, 17] indicate that the α-mode will lie below the frequency window for the given temperature range, whereas the β- and γ-modes will lie above it. The higher magnitude loss peak of [5] may have been caused by the ingress of water into the cable or because the Frequency Response Analyzer was attempting to measure below its sensitivity limit.

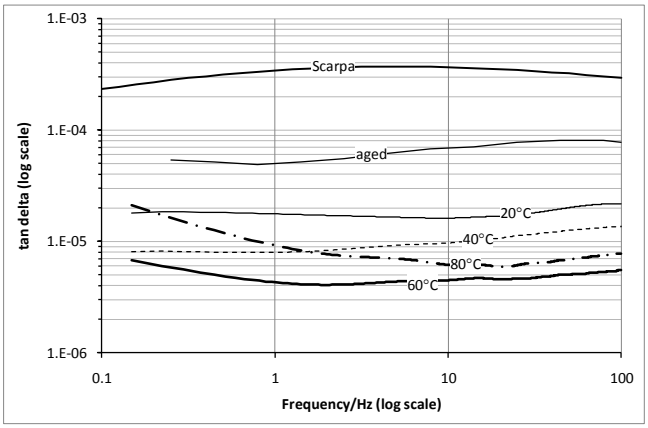

Figure 17: Dielectric loss due to polarization at mid-range frequencies at different temperatures in comparison with Scarpa *et al* [5]

The temperature behavior is consistent with an interpretation of the response in terms of a β-mode peak lying above the frequency window and an α-mode peak lying below the window. As shown in [16,17] the β-mode response is rather weak and its peak should lie well above 100Hz at all the measurement temperatures. As the temperature increases from 20°C upwards this peak will move to higher frequencies (activation energy about 0.5 eV) and its contribution to the dielectric loss in the measured frequency range will reduce. At 20°C and 40°C the α-mode response peak will lie at very much lower frequencies than the frequency window, however its activation energy (~1 eV) is much larger than that of the β-response and the high frequency tail of this stronger response mode will enter the window at the higher temperatures of 60°C and 80°C as seen in Figure 16. The same behavior is found in some previously unpublished data obtained by Borealis using a Schering Bridge at 50 Hz and 25 kV/mm, Figure 18. The tanδ measured by Borealis is somewhat higher, and this is likely to be related to the much higher electric field.

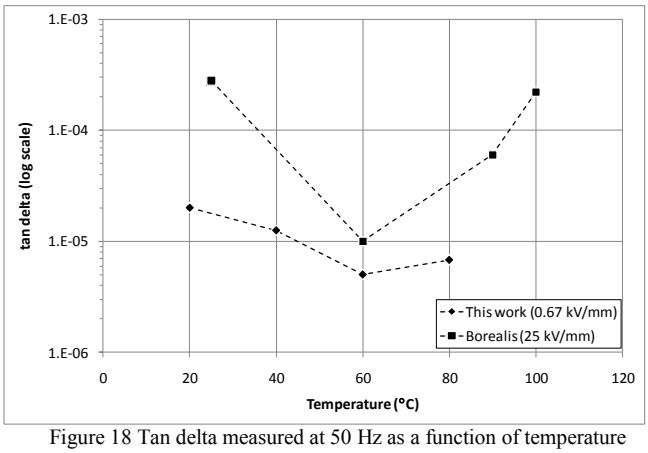

Figure 18 Tan delta measured at 50 Hz as a function of temperature measured at low field (this work) and by Borealis using a Schering Bridge at higher electric fields.

Figure 17 also shows the tanδ of the aged cable in this frequency range measured at 80°C. The ageing has increased the dielectric loss by about an order of magnitude although, in absolute terms, the tanδ is still very low. This data indicates that the thermal ageing has increased the magnitude of the β-mode response, and just possibly reduced its peak frequency. The ageing also seems to have increased the α-mode response. Such changes can be related to changes in the polyethylene morphology as discussed below.

Polyethylene is a partially crystalline material. The polymer chains may arrange themselves into crystalline sheets known as lamellae (e.g. [18]) which are surrounded by waxy amorphous (i.e. non-crystalline) regions. This amorphous region will contain impurities and additives, imperfect polymer chains (e.g. crosslinking branches) and chains that link adjacent lamellae. The β-response is the result of the motion of chain segments in the amorphous region. An overall reduction of density via the generation of free volume in the amorphous region would lead to an increase of 'fluidity' in the amorphous region and an increase of the strength of the β-mode response. The strength of γ-mode response, which lies at very high frequencies, would not change much as it is caused

by kink or crankshaft motions that are facile even in the constrained conditions of the glassy polymer. The α-polarization response is produced by twists of chains in the crystal lamella [17] accompanied by an elongation to retain matching with neighboring chains of the crystal. Disordering of the lamella-amorphous interface caused by increases to the free volume in the amorphous region would favor the possibility of such motions and lead to an increase of the strength of this response, though a dissolving of the smaller and more unstable lamella would tend to reduce its dielectric loss strength. It therefore seems that the high temperature of the thermal ageing allows a greater freedom of movement of chains in the amorphous region and probably unraveled some of the smaller lamella. The increased chain displacements have resulted in a greater free volume and disordered lamella surfaces when the cable was subsequently cooled for the dielectric response measurements.

D. Higher Frequency Behavior

It can be seen from equ. (5), that $\tan\delta \to R_S C\omega$ at higher frequencies. We would therefore expect the tanδ to be proportional to the series resistance of the semicon. The semicon DC resistivity was measured as a function of temperature and this can be seen to have the same trend as that of tanδ at 10 kHz in Figure 19. This is therefore consistent with the explanation that the higher frequency behavior of tanδ is dominated by the series resistance of the semicon layers.

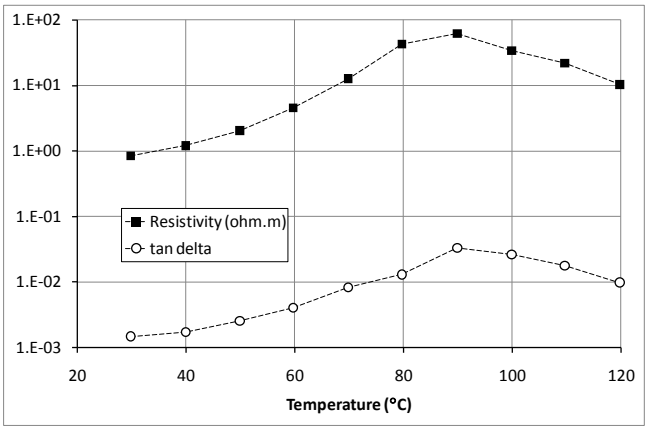

Figure 19: Cable tanδ at 10 kHz and semicon resistivity

CONCLUSIONS

The dielectric response of the XLPE power cables studied, can be modeled as a resistance due to the total resistance of the semicons, in series with a parallel combination of DC conductance of the XLPE insulation and the its capacitive response. The DC conductivity is very difficult to measure and the development of a bespoke noise-free supply was necessary to achieve this satisfactorily. The two measurement techniques of low-frequency dielectric spectrometry and of using a bespoke ultra-low-noise power supply showed excellent agreement with conductivities of 10^{-17} S.m^{-1} at 40°C. Extrapolation on an Arrhenius plot to room temperature would imply a conductivity of ~10^{-17} S.m^{-1}; this is lower than has been measured before. The activation energy of the conductivity was ~1.1 eV, however without degassing the cable there is a significant contribution to the conductivity dominated by impurities with a higher activation energy (~1.4 eV), suggesting they may be ionized antioxidants or crosslinking byproducts.

Below 1 Hz the dielectric response is dominated by this parallel DC conduction and above 100 Hz it is dominated by the series resistance of the semicons. The window between these two processes affords a glimpse of the polarization processes of the XLPE. This is a very broad low-loss process with a tanδ<10^{-5}. It is believed that that there is an α-mode relaxation process below the frequency window produced by the twists in the chains in the crystalline region. There may also be a β-mode relaxation at higher frequencies, the result of the motion of chain segments in the amorphous region.

Whilst both the tanδ and the conductivity are difficult to measure, it is felt that such measurement may be contribute to the assessment of aging of such cables; an assessment which is acknowledged to be notoriously difficult.

ACKNOWLEDGMENT

The University of Leicester gratefully acknowledges the support of Borealis AB through the provision of a PhD scholarship for Tong LIU.

REFERENCES

[1] J C Fothergill and R N Hampton, “Polymer Insulated Power Cable” in Advances in High Voltage System” M Haddad and D Warne (eds),: IEE 2004, pp. 495-528

[2] http://www.nationalgrid.com/NR/rdonlyres/C9AF5612-DF25-4FCF-ABB5-69F237ACB0C5/3411/SPTTS25.pdf (accessed 01 January 2011)

[3] J.C.Fothergill: “Electrical Insulation Systems for a Sustainable Energy Society” Invited opening paper for the 21st Nordic Insulation Symposium, Chalmers University of Technology, Sweden, June 15-17 2009

[4] L.A. Dissado and J.C. Fothergill, Electrical Degradation and Breakdown in Polymers, Peter Peregrinus Ltd. for the IEE, 1992

[5] P.C.N. Scarpa, A. Svatik, and D.K. Das-Gupta. “Dielectric spectroscopy of a polyethylene in the frequency range of 0.00001 Hz to 100000 Hz.” Polymer Engineering and Science, vol. 36(8), pp. 1072–1080, 1996

[6] http://www.kayelaby.npl.co.uk/chemistry/3_11/3_11_1.html (accessed 02 December 2010)

[7] J. Densley, "Ageing and diagnostics in extruded insulations for power cables," in Proceedings of the 1995 IEEE 5th Int Conf on Conduction and Breakdown in Solid Dielectrics, pp.1-15

[8] T. Liu, J.C. Fothergill, S.J. Dodd, U.H. Nilsson, “Influence of Semicon Shields on the Dielectric Loss of XLPE Cables”, IEEE Conference on Electrical Insulation and Dielectric Phenomena, USA, pp. 246-249, Oct 2009

[9] T Liu, J C Fothergill, S J Dodd, L A Dissado, “Dielectric spectroscopy study of thermally-aged extruded model cables” 2010 IEEE International Conference on Solid Dielectrics, Potsdam, Germany, pp 16-19,

[10] M. Nedjar, “Effect of thermal aging on the electrical properties of crosslinked polyethylene”, J. Appl. Polym. Sci., Vol. 111(4), pp. 1985-1990, (2009)

[11] T. Liu, J.C. Fothergill, S.J. Dodd, U.H. Nilsson, “Dielectric Spectroscopy of XLPE Cables using Discharging Current Measurement” IET INSUCON 2009 Conference, Birmingham, 26 – 28 May 2009

[12] N. Hozumi, T. Takeda, H. Suzuki, T. Okamoto, "Space charge behavior in XLPE cable insulation under 0.2-1.2 MV/cm dc fields,"

IEEE Transactions on Dielectrics and Electrical Insulation, vol.5(1), pp.82-90, Feb 1998
[13] J.C. Fothergill, K.B.A See, M.N. Ajour, L.A. Dissado, ""Sub-hertz" dielectric spectroscopy," in Proceedings of IEEE 2005 International Symposium on Electrical Insulating Materials, vol.3, pp. 821- 824
[14] B. Garros, "Ageing and reliability testing and monitoring of power cables: Diagnosis for insulation systems, The ARTEMIS program" IEEE Electrical Insulation Magazine, vol 15(4), pp 10-12 (1999)
[15] A.K. Jonscher, "Dielectric Relaxation in Solids", Chelsea Dielectric Press, London, (1983)
[16] J-P. Crine, "Rate Theory and Polyethylene Relaxations, IEEE Transactions on Dielectrics and Electrical Insulation, vol.22, pp169-174, 1987
[17] R.H.Boyd, " Strengths of the Mechanical α- β- and γ- relaxation processes in linear polyethylene", Macromolecules, vol.17, pp. 903-911, 1984
[18] R.H.Boyd, "Relaxation processes in crystalline polymers: Molecular interpretation---a review", Polymer, vol.26, pp. 1123-1133, 1985

John C. Fothergill (SM'95, F'04) was born in Malta in 1953. He graduated from the University of Wales, Bangor, in 1975 with a Batchelor's degree in Electronics. He continued at the same institution, working with Pethig and Lewis, gaining a Master's degree in Electrical Materials and Devices in 1976 and doctorate in the Electronic Properties of Biopolymers in 1979. Following this he worked as a senior research engineer leading research in electrical power cables at STL, Harlow, UK. In 1984 he moved to the University of Leicester as a lecturer. He now has a personal chair in Engineering and is Head of the Department of Engineering.

Tong Liu, born in 1980, obtained his Bachelor's degree in electrical engineering in 2003 and Master's degree in high voltage and insulation technology in 2006 at Xi'an Jiaotong University in China. With a UK government scholarship, he studied for a PhD at the University of Leicester, UK and obtained his PhD in 2010. During his research, he focused on dielectric response, partial discharge, surface flashover and space charge studies on power equipment, e.g. XLPE power cables and power transformers. He is now working as a researcher in EPRI of China Southern Power Grid (CSG). His main research interests are testing and operation technology of all high voltage power equipment, including power transformer, breakers, GIS, arrester, power cables and insulators.

S.J.Dodd was born in Harlow, Essex in 1960. He received the B.Sc. (Hons) Physics degree in 1987 and the Ph.D. degree in physics in 1992, both from London Guildhall University, UK and remained at the University until 2002 as a Research Fellow. He joined the University of Southampton in 2002 as a Lecturer in the Electrical Power Engineering Group in the School of Electronics and Computer Science and then the University of Leicester in the Electrical Power and Power Electronics Research Group in the Department of Engineering in 2007 as a Senior Lecturer. His research interests lie in the areas of light scattering techniques for the characterization of polymer morphology, electrical treeing breakdown process in polymeric materials and composite insulation materials, electroluminescence and its relationship with electrical and thermal ageing of polymers, characterization of liquid and solid dielectrics and condition monitoring and assessment of high voltage engineering plant. He has published 23 papers, 47 conference papers and contributed to two books.

Leonard A Dissado: (F'2006). Born: St .Helens, Lancashire, U.K 1942. Graduated from University College London with a 1st Class degree in Chemistry in 1963 and was awarded a PhD in Theoretical Chemistry in 1966 and DSc in 1990. After rotating between Australia and England twice he settled in at Chelsea College in 1977 to carry out research into dielectrics. His interest in breakdown and associated topics started with a consultancy with STL begun in 1981. Since then he has published many papers and one book, together with John Fothergill, in this area. In 1995 he moved to The University of Leicester, and was promoted to Professor in 1998. He has been a visiting Professor at The University Pierre and Marie Curie in Paris, Paul Sabatier University in Toulouse, Nagoya University, and NIST at Boulder Colorado. He was awarded the degree of Docteur Honoris Causa by the Université Paul Sabatier, Toulouse, France, in October 2007, and was made a Honorary Professor of Xian Jiaotong University, China, in September 2008.

Ulf Nilsson was born in 1961. He received his Master of Science degree in engineering physics in 1987 at Lund Instutute of Technology (Sweden). The focus was solid state physics especially solicon-based semiconductive technology. He joined Neste Polyeten AB in Stenungsund north of Gothenburg in 1987 responsible for electrical testing of polyethylene compounds for wire & cable applications. This company later became part of the Borealis group. He is currently engaged in product development of power cable compounds and activities related to improved understanding of the performance of insulating and semiconductive materials under high ac and dc electric stress.